A Method for Dihedral Angle Measurement in Solids: Rotational Resonance NMR of a Transition-State Inhibitor of Triose Phosphate Isomerase

York Tomita,† Edward J. O'Connor,†,‡ and Ann McDermott*,†

Contribution from the Department of Chemistry, Columbia University, New York, New York 10027, and Chemical Research and Development, Sandoz Research Institute, East Hanover, New Jersey 07936

Received January 24, 1994®

Abstract: In rotational resonance, a solid-state NMR technique for measuring dipolar couplings, the spinning speed, ν_r, is adjusted such that $\Delta\nu_{iso} = n\,\nu_r$, where $\Delta\nu_{iso}$ is isotropic chemical shifts difference and n (an integer) is referred to as the order. At higher orders of the rotational resonance the magnetization exchange rate depends strongly upon the relative orientations of the two carbons, particularly if both sites have broad chemical shift anisotropy. Experimental exchange curves and computer simulations for crystalline [$^{13}C_2$]glycolic acid at $n = 4$ demonstrate that this effect can be used to measure dihedral angles. Our data indicate that the hydroxyl group and the two carboxyl oxygen atoms are in the same plane, in agreement with crystallography. Phosphoglycolic acid (PGA) is a transition-state analog inhibitor of triose phosphate isomerase (TIM). The $n = 4$ exchange curves for [$^{13}C_2$]PGA bound to TIM indicate an "in-plane" conformation for the phosphate with respect to the carboxy group. This conformation had been previously proposed to explain the lack of phosphate elimination during catalysis and had been suggested also on the basis of crystallographic results. The chemical shift anisotropy of the carboxy group of PGA indicates that it is deprotonated when bound to the enzyme. We discuss the scope of applications of rotational resonance for measuring dihedral angles in other systems.

Introduction

Recent progress in solid-state NMR techniques introduced the possibility of measuring chemically interesting parameters like chemical shift anisotropies, anisotropic relaxation parameters, and hetero- and homonuclear dipole couplings in complex solids. In solution, dipole–dipole couplings are substantially averaged due to fast tumbling of molecules and do not affect the line shapes. The dipolar interactions can be more apparent in solid-state NMR spectra, and recently rather long-distance dipolar couplings involving selectively introduced heteroatoms have been observed using rotationally enhanced double resonance (REDOR),[1] rotational resonance (RR),[2] and other methods.

Rotational resonance for a dilute homonuclear spin pair occurs if the spinning speed (ν_r) is matched to the difference in isotropic chemical shifts ($\Delta\nu_{iso}$) to satisfy the condition

$$\Delta\nu_{iso} = n\,\nu_r$$

in which the integer n is the order of rotational resonance. At these spinning speeds, the the zero-quantum transition for the spin pair is strongly excited and an oscillatory exchange profile of Zeeman magnetization between the dipolar-coupled spins may be measured. For especially strong couplings the resonance lines can be broadened or split. Numerical simulations of these profiles permit the determination of the internuclear distances with high accuracy. Previous rotational resonance experiments showed that this technique could be used to measure distances as large as 6 Å even for very dilute homonuclear spin pairs in biological systems.[3] In those cases, the $n = 1$ condition was employed to yield a frank measurement of the distance without effects of the dihedral angles.

Rotational resonance at higher orders ($n > 3$) is sensitive to the relative orientation of the two tensors, especially when both sites have rather large shift anisotropy. To clarify this point, we illustrate in Figure 1 the origin of rotational resonance; the principles governing this effect have been amply discussed previously, but we have reformulated it in a schematic and graphical fashion. For the solution NOE or for rotational resonance, zero-quantum transitions are excited by fluctuations in the dipolar Hamiltonian whose spectral density matches the frequencies in the zero-quantum spectrum. In solution the zero-quantum spectrum consists of a simple line at the difference of the two isotropic shifts—for two protons this frequency would typically be a few kilohertz. Spectral density in the dipolar fluctuations at these low frequencies is always provided by the random tumbling of the molecule. In the solid-state during magic angle spinning, the zero-quantum spectrum will generally include a peak at the difference frequency for the two sites (as occurs for solution spectra) but also contain spinning sidebands around that frequency. The strengths of these sidebands depend on the chemical shielding anisotropies and the relative orientations of the two groups, as is described in Figure 1. The main source of fluctuations in the low-kilohertz range for solids during magic angle spinning is the rotation of the sample. This simple rotation at a fixed frequency modulates the dipolar Hamiltonian; since the dipolar Hamiltonian depends specifically on $\cos^2\Theta$, the correlation function or spectral density of dipolar fluctuations has sharp features at ν_r and $2\nu_r$. The rate of zero-quantum transitions may therefore be controlled by selecting the spinning speed either to match a zero-quantum centerband, to match a sideband, or to miss all of the features. For example, Figure 1

† Columbia University.
‡ Sandoz Research Institute.
* Abstract published in *Advance ACS Abstracts*, August 1, 1994.

(1) (a) Gullion, T.; Schaefer, J. *J. Magn. Res.* **1989**, *81*, 196–200. (b) Gullion, T.; Schaefer, J. *Adv. Magn. Reson.* **1989**.

(2) (a) Raleigh, D. P.; Levitt, M. H.; Griffin, R. G. *Chem. Phy. Lett.* **1988**, *146*, 71. (b) Levitt, M. H.; Raleigh, D. P.; Creuzet, F.; Griffin, R. G. *J. Phy. Chem.* **1990**, *92* (11), 6347.

(3) (a) Creuzet, F.; McDermott, A. E.; Gebhard, R.; van der Hoef, K.; Spijker-Assink, M. B.; Herzfeld, J.; Lugtenburg, J.; Levitt, M. H.; Griffin, R. G. *Science* **1990**, *251*, 783–785. (b) McDermott, A. E.; Creuzet, F.; Griffin, R. G.; Zawadzke, L. E.; Ye, Q.-Z.; Walsh, C. T. *Biochemistry* **1990**, *29*, 5767–5775. (c) McDermott, A. E.; Creuzet, F.; Gebhard, R.; Levitt, M.; van der Hoef, K.; Lugtenburg, J.; Herzfeld, J.; Griffin, R. G. *Biochemistry* **1994**, *33*, 6129–6136. (d) Thompson, L. K.; McDermott, A. E.; Raap, J.; van der Wieleden, C. M.; Lugtenburg, J.; Herzfeld, J.; Griffin, R. G. *Biochemistry*, **1992**, *31*, 7931–7938.

0002-7863/94/1516-8766$04.50/0

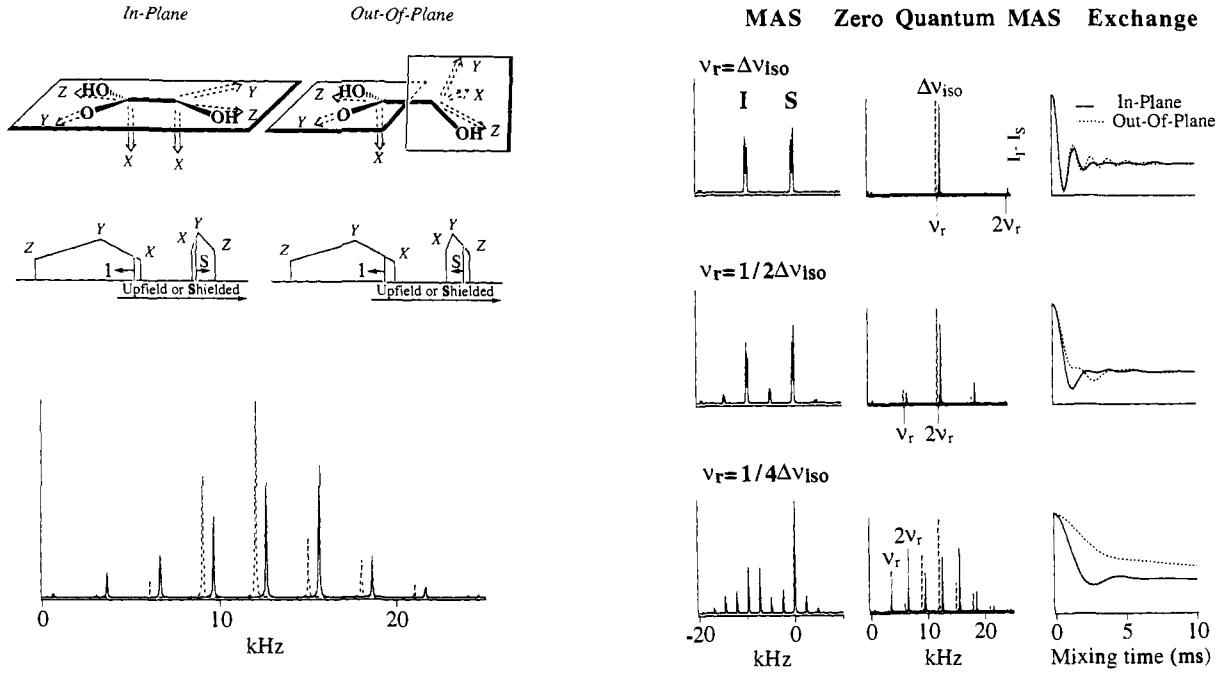

Figure 1. (Left) Schematic representations of in- and out-of plane conformations of a molecule such as glycolic or phosphoglycolic acid with its corresponding powder patterns. On the structure the directions of the tensor elements are shown. On the powder pattern the resonance frequencies are shown for the specific crystallites in which the magnetic field is along the x axis (most shielded direction) for the carboxy group (most shielded axis). The small arrows indicate the sense in which the resonance frequencies would change during sample rotation. The *difference CSA*, defined as the anisotropic difference in the two carbon frequencies as a function of orientation with respect to the static magnetic field, is substantially larger for the in-plane than for the out-of-plane conformation, and the difference frequency for the two sites accesses a broad range of values during magic angle spinning. This oscillating difference frequency gives rise to stronger sidebands in the zero-quantum spectrum of the in-plane conformer, as shown below with the solid ZQ MAS spectrum with stronger sidebands representing the in-plane spectrum and the dashed spectrum with the small sidebands representing the out-of-plane spectrum. (Note that for clarity the values used in these simulations are slightly exaggerated as compared with those in table 1, so Figure 1 is a schematic only. Figures 2, 3, and 5 on the other hand utilize the values in Table 1.) (Right) Comparison of three orders of rotational resonances for the parameters appropriate for a molecule such as glycolic acid or phosphoglycolic acid. On the left the MAS ("single-quantum") spectra are shown; the dipolar fine structure of these spectra would in fact depend upon tensor orientation but cannot be seen in the figure. In the center the zero quantum MAS spectra are shown for both the in-plane (solid line) and out-of-plane (dotted line) conformers. "Tics" below the axis indicate the only frequencies at which sample rotation would introduce spectral density in the modulation of the dipolar coupling, that is the rotation frequency and twice that frequency. Exchange between the two sites depends rigorously on overlap between the zero-quantum spectrum and the spectral density for dipolar modulation. For the $n = 1$ and $n = 2$ conditions, there is no great distinction in this overlap between the in-plane and out-of-plane conformations because the centerband intensity of the MAS spectrum is responsible for most of the exchange. In contrast, for the $n = 4$ condition the exchange is entirely due to overlap between the spectral density and the MAS sidebands. As discussed above, these sideband intensities are quite different for the in-plane and out-of-plane conformations so that the $n = 4$ exchange curve is much faster if the molecule is in-plane. On the right the calculated exchange curves for in-plane and out-of-plane conformers are shown.

shows that the $n = 1$ condition is driven by the overlap between the zero-quantum centerband at $\Delta\nu_{iso}$ and the dipolar fluctuation at ν_r.

The $n = 4$ condition requires overlap between a zero-quantum sideband and ν_r or $2\nu_r$. The formation of zero-quantum sidebands in turn relies on *difference chemical shielding anisotropy* (*CSA*); i.e., they are produced by the oscillating difference in the anisotropic part of the chemical shift during magic angle spinning (MAS). For example Figure 1 illustrates that for the out-of-plane conformation of glycolic acid (GA) the most shielded direction for the I spin is in the same physical direction as the most shielded direction for the S spin. In this case the two spins travel in the same sense through their respective tensors and sideband formation is relatively weak. In contrast, if the dihedral for the bond is rotated to form the in-plane conformer, then the most shielded direction for the I spin corresponds to the least shielded direction for the S spin. In that case, during MAS they travel in contrary senses through their respective tensors and their difference frequencies or zero-quantum frequencies will be very strongly modulated. Consequently, strong sidebands will be generated for this in-plane conformation of glycolic acid. These spectral features will overlap the components of the rotor rotation spectral density at $n = 4$, and zero-quantum transitions are excited. In summary the intensity of the zero-quantum sidebands depends systematically on the dihedral angle and the exchange rates at $n = 4$ are thus sensitive to this dihedral angle as well.

Usually the dihedral angles could also be estimated from the Karplus relationship when both sites have directly bound protons. However the cases we describe in this report would not be amenable to analysis by a Karplus relationship because the proteins are very large and one of the carbons in the bond has no attached proton or other NMR-active nucleus.

The parameters required for the numerical simulations of rotational resonance include the distance, the complete chemical shift anisotropies, and the orientations of tensors. The orientations of carbon CSA tensors for most typical chemical groups have been determined in relation to the crystal structural axes by single-crystal rotation studies.[4] Typically the magnetic shielding axes are readily transferable from one molecule to another of similar structure and many have been calculated by *ab initio* methods. The zero-quantum transverse relaxation time, T_2^{ZQ}, or zero-quantum line width must also be known. Currently we estimate this by convolving the two single-quantum values for T_2 corresponding to the two members of the pair, which are in turn estimated from the line widths. Since the $n = 1$ or $n = 2$ exchange curves are essentially independent of dihedral angle, we measure the $n = 2$ curve and check the quality of the simulation to confirm that all parameters other than the dihedral angle are correct. Ideally one would measure $n = 1$ also if the experimental apparatus allows for high-speed spinning.

(4) Veeman, W. *Prog. NMR Spectrosc.* **1984**, *16*, 193–235.

The application of rotational resonance for measurement of dihedral angles had been proposed in earlier publications.[3] This report constitutes the first clear demonstration of such a measurement done both on a crystalline small molecule and on a ligand to a 50-kDa protein, the transition-state analog compound phosphoglycolic acid (PGA) bound to triose phosphate isomerase (TIM). In addition we discuss the scope of the method for other problems in structural biology.

Materials and Methods

[$^{13}C_2$]Glycolic acid and phosphoglycolic acid were prepared as described elsewhere (O'Connor et al., 1994). Glycolic acid was recrystallized by slow evaporation from an aqueous solution in the presence of a desiccant. Triose phosphate isomerase was expressed and purified as will be described in a future publication (Tomita et al., unpublished). Sixty milligrams of the enzyme was obtained and combined with labeled PGA in a one to one ratio on the basis of active sites. The enzyme–inhibitor complex was then rapidly frozen and lyophilized until it "barely" formed a solid and was loaded into an NMR rotor. These samples gave very broad spectra (ca. 4–6 ppm line widths). In another experiment we precipitated the enzyme using polyethylene glycol; the resulting line widths are much narrower (2 ppm), and those spectra are shown in Figures 5 and 6. The samples were prepared from comercial yeast TIM (Sigma) in 10 mM Tris, 1 mM EDTA, 1 mM mercaptoethanol, 20 mM KCl, 30% PEG 3400 (Aldrich) and were incubated and centrifuged to obtain a pellet at 4°C, containing approximately 40 mg of protein. After measuring the "empty" enzyme, an approximately equimolar amount of [$^{13}C_2$]-PGA was dissolved in a similar buffer and added to the mother liquor in the rotor. This was allowed to soak into the crystals for 2 h before measurement. The measurements were made at 10 ± 1°C. We have studied the kinetics of TIM microcrystals in the presence of precipitants, and the use of polyethylene glycol preserved normal kinetic parameters (unpublished). We estimate k_{off} for this compound to be >10 s^{-1} at 10 °C, which is long on our experimental time scale.

All the spectra were taken on a Chemagnetics CMX400 operating at 99.71 MHz for ^{13}C and 396.5 MHz for ^{1}H. The pulse sequence used was similar to that described previously [3a] with a modification for background signal suppression[5] and an improved phase cycling. In addition a variable delay time was added before the selective inversion pulse to result in a constant time experiment. The latter modification resulted in noticeably improved difference spectra. Typical experimental conditions involved ^{1}H and ^{13}C 90° pulses of 4 μs, a 3-ms cross-polarization pulse, a 180-μs ^{13}C 180° pulse for the selective inversion, a 18-ms acquisition time, and a 20-s recycle delay. The decoupling power was adjusted to the point where a higher decoupling power did not provide any significant improvement in the line width. Spectra were collected in sets of 20 with mixing times starting from 100 ns as a zero mixing time, which was used to normalize the data set. The mixing times were randomly scrambled to average out the spectrometer instability, and 32 transients were accumulated for each mixing time. Magnetization transfer data were obtained by integrating over all the sidebands of the each site of resonance and then correcting for zero mixing time and the natural abundance ^{13}C background signal. Analysis of the glycolic acid data by use of the intensities of the centerbands gave very similar results.

Because of a difference in chemical shift for the two glycolic acid molecules in the unit cell (see results), resonance conditions between 2926 and 3018 for $n = 4$ might be conceivable. The strongest exchange curves were detected at speeds of 2958 for $n = 4$ and 5916 for $n = 2$, and all reported data were collected at these spinning speeds. The selective inversion pulse (carbon-180 of ~180 μs) "covers" both methylene resonances without discriminating between these two. Experiments with off-resonance conditions were also conducted for both $n = 2$ and 4 (data not shown). In these experiments, the spinning speed was displaced by about 200 Hz from the resonance condition, an offset somewhat larger than the full width at half maximum (fwhm) line width. No evidence of exchange was observed for mixing times up to 10 ms.

The data reported for PGA on TIM were also measured as integrated intensities taken from a labeled-minus-unlabeled difference spectrum. Rotational resonance at the $n = 2$ and $n = 4$ resonance orders corresponding to the spinning speed at 5616 and 2808 Hz, respectively, was performed and processed in a similar manner as for glycolic acid. Approximately 5000–10 000 transients were added for each spectrum.

Simulations of the exchange curves were calculated using a previously described program.[2b] For Figure 1, the zero-quantum chemical shielding tensor elements for each spin pair were calculated by first applying the rotations to each chemical shift tensor (that were selected on the basis of the conformation and knowlege of the orientations of the tensors in the molecular frame), computing the difference CSA and then diagonalizing the resulting difference tensor. The corresponding MAS spectra were then calculated by numerical simulation of the equations of motion for the magnetization under the influence of a time-dependent Hamiltonian and powder averaging. The same formulation that typically describes a single-quantum MAS spectra for three tensor elements was used.

Results and Discussion

Cross-polarization with magic angle spinning (CP-MAS) spectra of glycolic acid show a small difference in σ_{iso} which we attribute to the two crystallographically nonidentical molecules seen in a diffraction experiment. The differences in conformation between these molecules are very small,[6] involving a difference in bond distances of approximately 0.01 Å and in the dihedral angle of 3.4°. The two molecules gave almost identical chemical shift anisotropies except for the small offset and the fact that the chemical shielding anisotropy analysis indicates that both molecules are protonated on the carboxyl group. In the following rotational resonance experiments, the two peaks were averaged together and a single exchange profile is presented.

Figure 2 shows the exchange curves as well as simulations for the second resonance order ($n = 2$). The parameters used in these simulations are listed in Table 1. With the discussion of the orientations of the tensors, all parameters are known from independent measurements on these compounds. The simulations of magnetization exchange for glycolic acid utilize a dihedral angle of 2.4° (taken from X-ray crystal data to describe the in-plane conformation) and 90° (a hypothetical out-of-plane conformation). The Euler angles for the carboxylic acid were determined assuming that the most shielded direction is orthogonal to the sp^2 plane and the intermediate one is close to the carbonyl but rotated approximately 15° toward the C–O single bond. For the methylene, the most shielded direction is close to the C–O bond and the intermediate one is the plane perpendicular to the C–O bond but closest to the carbon–carbon bond. Both assumptions were based on previously determined values for alcohols and carboxylic acids.[4] The experimental value for the J coupling (59 Hz) was utilized, and the dipolar coupling constant (2.26 kHz) was calculated from a crystallographic bond distance of 1.498 Å without correction for Debye–Waller thermal disorder factors. The values of the chemical shielding anisotropy tensors were measured from the low spinning (1700 and 2000 Hz) MAS spectra with standard computer sideband fitting analysis. Estimates for T_2^{ZQ} based on the line width, $(T_2^{ZQ})^{-1} = (T_2^{(I)})^{-1} + (T_2^{(S)})^{-1} = \pi(\delta_{(I)} + \delta_{(S)})$, where δ is the half-height line width, have been previously shown to be reliable for our purposes,[3a] and this method gives a value of 0.6–0.8 ms for crystalline glycolic

(5) Bax, A. *J. Magn. Reson.* **1985**, *65*, 142.

(6) (a) Pijper, W. P. *Acta Crystallogr.* **1971**, *B27*, 344. (b) Ellison, R. D.; Johnsons, C. K.; Levy, H. A. *Acta Crystallogr.* **1971**, *B27*, 333.

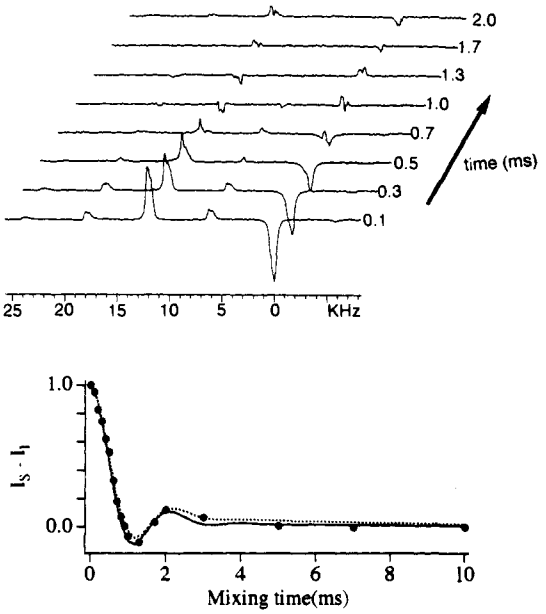

Figure 2. Measured magnetization exchange for glycolic acid at the $n = 2$ condition. (Top) Stack plot of spectra with variable mixing times, τ, as indicated. In each case, the methylene resonance region was selectively inverted by a weak pulse. (Bottom) Exchange simulations for in-plane (solid) and out-of-plane (dotted) conformations presented with experimental data. The difference in integrated peak intensities ($I_I - I_S$), normalized to 1 at zero mixing time, is plotted as a function of mixing time. The parameters used for the simulations are indicated in Table 1.

Table 1. Parameters Used in Simulations in Figures 2–5[a]

sample	glycolic acid	PGA on TIM
methylene		
CSA: $\sigma 11, \sigma 22, \sigma 33, \sigma_{iso}$ (ppm)	88, 68, 20, 58	98, 65, 32, 65
Euler angles (deg)		
in plane (α, β, γ)	90, 58, 92.4	90, 58, 92.4
out of plane (α, β, γ)	90, 58, 0	90, 58, 0
line width	259	239
carboxyl		
CSA: $\sigma 11, \sigma 22, \sigma 33, \sigma_{iso}$ (ppm)	264, 158, 108, 177	241, 178, 115, 178
Euler angles (deg)		
in plane (α, β, γ)	90, −115, 90	0, −180, 0
out of plane (α, β, γ)	90, −115, 90	0, −180, 0
line width	126–260	208
T_2^{ZQ} (ms)	0.63–0.83	0.58
dipolar coupling (distance)	2.26 kHz (1.49 Å)	2.26 kHz (1.49 Å)

[a] The Euler angles for the dipolar axis were (0, 0, 0) in every case. The reference frame used for the calculation of the Euler angles is drawn in Figure 7.

acid. The calculated initial exchange rates for the in-plane and the out-of-plane conformations are almost identical despite the large dihedral angle difference.

Rotational resonance at higher orders in resonance ($n = 3$ or 4) is expected to provide very good sensitivity to the dihedral exchange due the difference in CSA, as described in the Introduction. Figure 3 shows the data and simulations for $n = 4$. The initial exchange rates were much slower for both in- and out-of-plane conformations at n = 4 compared to $n = 2$, as expected. In addition, the out-of-plane curve was much slower than that for the in-plane conformer, which is a direct result of the fact that, for this relative orientation of the carbons, the crystallites with a strongly shielded methylene site also have a strongly shielded carboxyl site and so the zero-quantum sidebands are smaller. In contrast, for the in-plane orientation, a larger difference in CSA results from the fact that the orientation with shielded carboxyl sites corresponds to deshielded methylene sites, so the two carbons traverse their respective CSA patterns in opposing senses through most of the rotor cycle. The experimental data plotted along with the simulations agree very well with the calculation for the in-plane conformation.

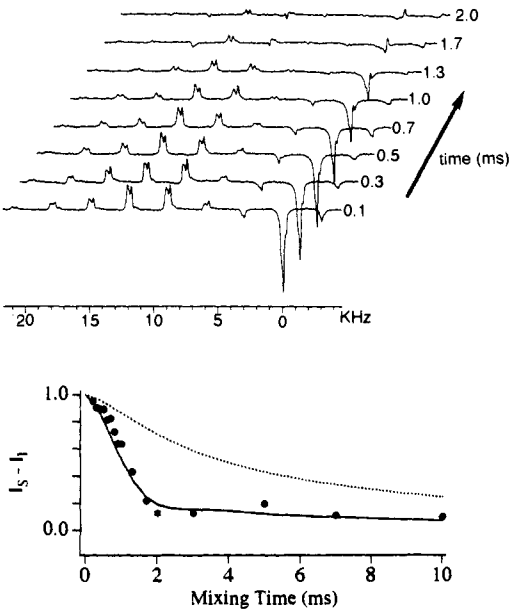

Figure 3. Measured magnetization exchange for glycolic acid at the $n = 4$ condition. (Top) Stack plot of spectra showing the exchange profile. (Bottom) Exchange simulations for in-plane (solid) and out-of-plane (dotted) conformations plotted with experimental data ($I_I - I_S$). The experimental data are within error of the in-plane simulated curve but not the out-of-plane curve. The parameters used for the simulations are indicated in Table 1.

Error analysis for the determination of the dihedral angle must include a consideration of the signal-to-noise ratio of the data as well as the covariance of the various simulation parameters. The values for these other parameters were estimated as described above (second paragraph of this section), are entered in Table 1, and were confirmed by measuring the $n = 2$ lower order of rotational resonance and simulating it successfully, as shown in Figure 2. To estimate the error that results from covariance in the parameters used in the fit at $n = 4$, "contour plots" of the error as a function of adjustable parameters were prepared for both orders of rotational resonance. In these plots, as explained in previous publications,[3c,d] two variable parameters in the simulation are systematically incremented (displayed in two dimensions on their respective axes) and the root mean square deviation between the corresponding simulation and the experimental data is the third dimension and is presented by means of contour level lines. We present plots involving parameters that are most important for simulating the $n = 4$ condition, namely the dihedral angle of interest which is effectively the Euler angle γ for the methylene site (S) and T_2^{ZQ}, the zero-quantum transverse relaxation parameter for the spin pair. The first plot illustrates that T_2^{ZQ} may be confirmed using the $n = 2$ data when the dipolar coupling is assumed to be known. The resulting choice of T_2^{ZQ} (0.60–0.65 ms) is within error of that estimated on the basis of line widths (0.6–0.8 ms) and is robust with respect to proposed values for dihedral angles. The second plot illustrates that the $n = 4$ data is quite sensitive to the dihedral angle but also to T_2^{ZQ}. When T_2^{ZQ} is assumed to be unknown and the global best fit minimum is examined, the dihedral angle is determined to be either $30 \pm 10°$ or $-30 \pm 10°$ and T_2^{ZQ} is determined to be >1 ms. This resulting dihedral value is in poor agreement with the crystallographically determined values of −2.4° and 5.8°, and the T_2^{ZQ} value is inconsistent with the line widths. If we constrain the value for T_2^{ZQ} to be 0.75 + 0.2 ms, then the area of best fit corresponds to a range of dihedral angles between −20 and 15°, in better agreement with crystallography. We conclude that an approximate estimation for T_2^{ZQ} is essential in these experiments and that the error range for the determination of the dihedral angle is rather large. We are currently attempting to develop direct methods for determining T_2^{ZQ}.

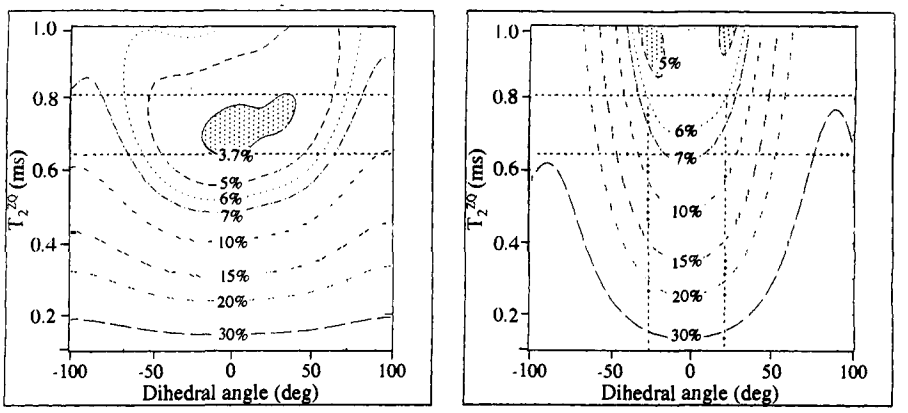

Figure 4. Contour plots displaying the dependence of root mean square deviation between various simulations and the exchange experiment when two parameters used in the calculations, T_2^{ZQ} and the dihedral angle (γ_S), are varied systematically. The areas of the minimum root mean square deviation are hatched, and other contour lines are drawn with the percentage root mean square deviation between data and simulation indicated. For $n = 2$, the dependence of fit quality on the T_2^{ZQ} value is quite strong and we use this measurement to confirm our value for T_2^{ZQ}. The dependence of this simulation on the dihedral angles was rather weak. The region of best fit is hatched and indicates values from 0.60 to 0.65 ms, and dihedral angles from −70 to 70° are acceptable. For $n = 4$, the dependence of fit quality on the dihedral angle (γ_S) is significant but the dependence of fit quality on the T_2^{ZQ} value is also quite strong. The global error minimum with no restriction on T_2^{ZQ} yields a range of values of 10–30°. When the experimental value for T_2^{ZQ} is imposed, the best fit region is indicated by the dotted line and yields a dihedral angle of 0 ± 20°. An approximate estimation of T_2^{ZQ} is therefore neccessary to obtain an accurate value for the dihedral angle. Other fit parameters for $n = 4$ have a much less significant effect, such as for example the polar angle for the carbonyl tensor (not shown).

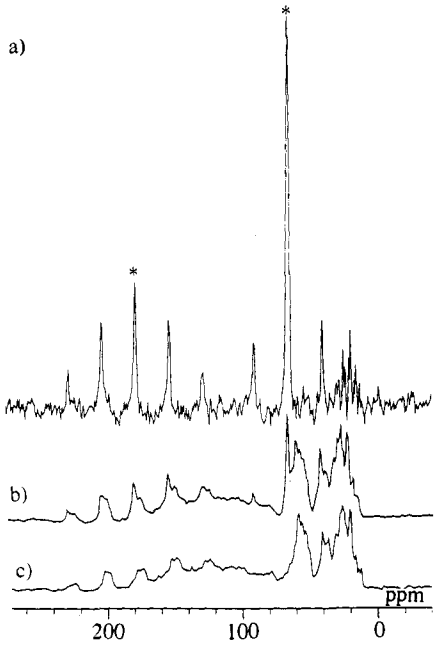

Figure 5. (Top spectrum, a) Low-speed (2.5 kHz) magic angle spinning labeled-minus-unlabeled difference spectrum of [$^{13}C_2$]PGA bound to TIM and precipitated using PEG. The simulation that is drawn over the spectrum utilizes the CSA values given in Table 1. (Middle spectrum, b) ^{13}C MAS spectrum of labeled PGA bound to TIM and precipitated with (30%) PEG. (Bottom spectrum, c) Corresponding unlabeled spectrum. The labeled and unlabeled spectra were processed (including phasing) separately and then subtracted using weighting factors based upon amount of sample and number of scans but then adjusted to obtain a high-quality baseline without artefacts from the backbone carbonyl and α carbon background.

We have confirmed that the several other Euler angles including the polar angle, β, for the carbonyl site (I) are unimportant for the simulation in this case and the values known from the single crystal studies in the literature result in good simulations of the data. Relatively large changes in these angles (20°) from their known values result in simulations that can be worse in the detailed fit to the curve, but the resulting range of acceptable dihedral angles is not significantly affected in the final analysis.

Figures 5 and 6 show the MAS difference (labeled-minus-unlabeled) spectrum and the exchange curves at $n = 2$ and $n = 4$ for a TIM-PGA complex precipitated from PEG, respectively. Chemical shift tensor values which are entered in Table 1 were obtained from a MAS spectrum and indicated, for the first time, that the carboxy group is deprotonated on the enzyme, by comparison with the known database for carboxy groups.[7] PGA is proposed to be a transition-state analog mainly on the basis of an assumed negative charge in the carboxy group; during catalysis negative charge is proposed to develop on the carbonyl of dihydroxyacetonephosphate, which would be located in an analogous location. Therefore confirmation of the ionization state of PGA substantiates the notion that it is a transition-state mimic.

The question of the conformation of this and other transition-state analog compounds at the active site of the enzyme has been discussed previously[8] and is quite relevant to control of reactivity on the enzyme. It has been pointed out that a preference on the enzyme for the "in-plane" conformation would predict stereoelectronic suppression of phosphate elimination during catalysis. Subsequently the crystal structures of the TIM–PGA complex indicated an "in-plane" conformation for PGA. Figure 6 displays the rotational resonance exchange curves for [$^{13}C_2$]PGA on TIM in PEG. The data points are the intensities of centerbands for labeled-minus-unlabeled difference spectra for the indicated mixing time. The solid curve is a calculation for an in-plane conformation, and the dotted line is for the out-of-plane conformation. The $n = 2$ data confirm our values for the T_2^{ZQ} and dipolar coupling for this sample. The $n = 4$ data confirm the previous suggestion that the in-plane conformation of this molecule is adopted on the enzyme. Therefore this approach to determination of dihedral angles appears to yield reliable results when applied to dilute systems, and our immediate goal is to measure conformations that are not accessible by crystallography, such as the Michaelis complex of DHAP on TIM. We display these results here to illustrate the ability of rotational resonance to characterize samples in a quantitative fashion even when they have a very low absolute number of spins (ca. 0.5 μmol).

A virtue of these analyses is that the parameters for simulation of the $n = 4$ data nearly all come from measurements on the same sample. Specifically, the CSA and the line widths are obtained from a set of MAS spectra, and the $n = 1$ or $n = 2$ spectra are used to confirm these values as well as the dipolar coupling. The exceptions are the dihedral angle(s), which we are attempting to

(7) Gu, Z.; McDermott, A. *J. Am. Chem. Soc.* **1993**, *115*, 4284.

(8) (a) Lolis, E.; Alber, T.; Davenport, R. C.; Rose, D.; Hartman, F. C.; Petsko, G. A. *Biochemistry* **1990**, *29*, 6609–6618. Lolis, E.; Petsko, G. A.; *Annu. Rev. Biochem.* **1990**, *59*, 597–630. (b) Wierenga, R.; Noble, M. E. M.; Postma, J.; Groendijk, H.; Kalk, K.; Hol, W.; Opperdoes, F. *Proteins: Struc., Func. Genet.* **1991**, *10*, 33–49, 50–69.

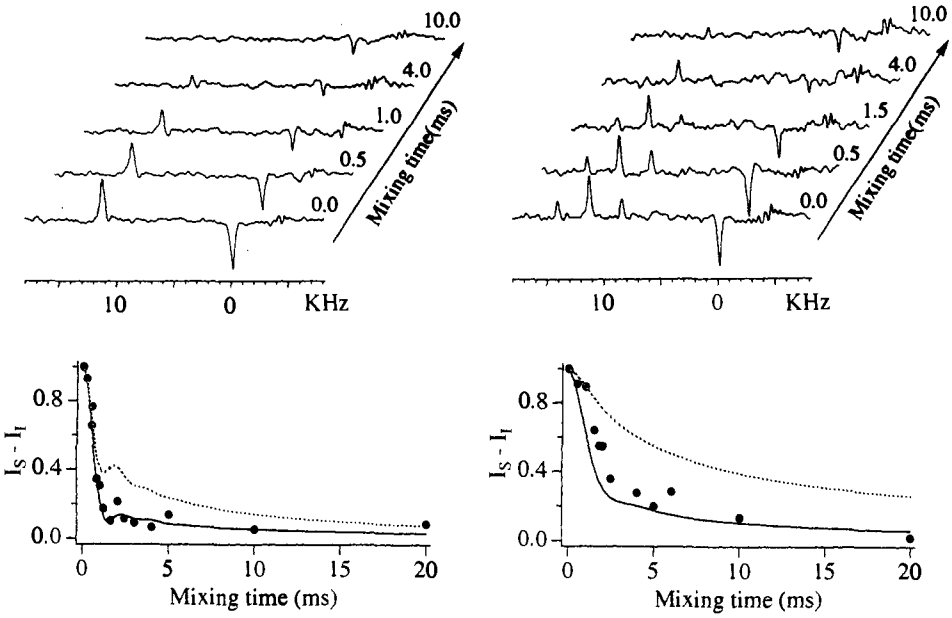

Figure 6. (Top) Experimental exchange spectra of ^{13}C-labeled PGA bound to TIM and precipitated with PEG. The exchange spectra are labeled-minus-unlabeled difference spectra. (Botom) Magnetization exchange curves for PGA on TIM at the $n = 2$ and $n = 4$ conditions with calculated curves utilizing the parameters in Table 1 for in-plane (solid) and out-of-plane (dotted) conformations. Parameters for the calculations are in Table 1.

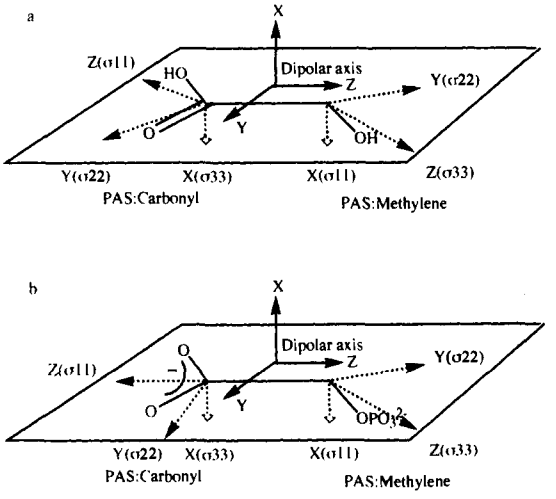

Figure 7. Coordinate system for calculation of the Euler angles in Table 1 and used for the simulations indicated pictorially. The directions for the shielding tensors of carboxyl groups are described in ref 7. For the methylene tensor we assumed that the most shielded axis is along the C–O bond and the intermediate axis is the vector perpendicular to the C–O bond that is closest to the C–C bond.

determine from the curve, and the orientations of the tensor elements, which are well-known in this example but must ultimately either be calculated or determined by rotation plots of model compounds.

We would like to comment briefly on the applicability of these methods to determination of dihedral angles in peptides and proteins. It is very important in this method that both carbons have rather broad tensors, so that the zero-quantum sidebands really reflect a correlation of the two sites and are not simply dominated by the spectrum of one site, as would happen for a compound with one broad and one narrow site. In addition this method fails for the special case that the most shielded element of the deshielded carbon (or else the least shielded element of the more shielded carbon) happens to coincide with the internuclear direction. A case of particular interest, the α and carbonyl carbons in a peptide, is unfortunately essentially dominated by the anisotropy of the carbonyl. In addition the deshielded element of the methylene site is quite close to the carbon–carbon vector, and so a precise value of the dihedral angle φ is not easily obtained by this method. When this method fails, probably any other solid-state NMR method for dihedral angle measurement will also be unsuccessful if it is ultimately based on mapping the chemical shift anisotropies.

Conclusions

Using glycolic acid as a model compound, we have demonstrated that rotational resonance can be used to measure dihedral angles for two directly bound carbons if they both have broad chemical shielding anisotropy. The higher order conditions are generally much more sensitive to the change in the dihedral angles than the lower orders $n = 1$ and $n = 2$. The angle determined with $n = 4$ data agreed well with the value known from x-ray crystal studies when experimental values for the relaxation time T_2^{ZQ} were included. Prediction of the dihedral angles within 20–30° is possible without very exacting determinations of the other parameters. We also demonstrate an extension of the technique to measurement of the dihedral angle for an inhibitor, PGA, bound to the enzyme TIM. This experiment illustrates the utility and robust nature of the method under challenging situations of low signal-to-noise ratios and significant background signals. On the other hand, for some situations of interest the rotational resonance curves might be relatively insensitive to dihedral angle, such as dihedral angles in a peptide backbone. The sensitivity of this method can be predicted quantitatively if the CSA values and their molecular orientations are known.

Acknowledgment. The authors would like to acknowlege Dr. Rik Wierenga of the EMBL in Heidelburg for useful discussions about the enzyme. We also thank Professor Robert Griffin and especially Dr. Malcolm Levitt, who wrote the program used for the simulations. Acknowledgement is made to the donors of The Petroleum Research Fund, administered by the American Chemical Society, for the partial support of this research. Y.T. and A.M. acknowledge support from the Kanagawa Academy of Science and Technology (KAST).